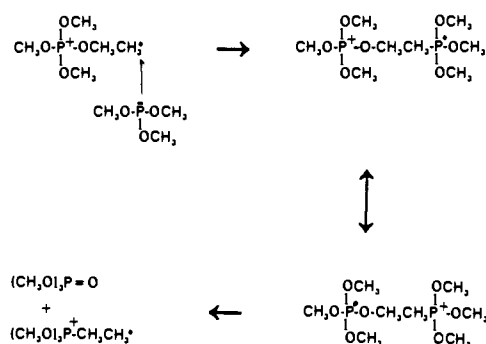


Scheme VI



The transfer of $C_2H_4^{•+}$ may involve a radical-type mechanism, perhaps via the hypervalent phosphorus radical intermediate depicted in Scheme VI. This proposal is supported by the results obtained for triethylamine and *sec*-butylamine that cannot generate an analogous intermediate radical: the distonic ion does not react at a measurable rate with these strong nucleophiles.

Conclusions

The reactivity of the first reported β -distonic radical cation that does not have acidic functional groups or unsaturation near the charge site differs from the behavior of most gaseous organic radical cations with a localized charge: no fast bimolecular reactions are observed for this ion. The fundamental reasons behind the observed resistance of this distonic ion to react with very strong bases, nucleophiles, and reductants are not clear at this time, although steric hindrance probably plays a role.¹⁵ Electron

(15) Meot-Ner, M.; Smith, S. C. *J. Am. Chem. Soc.* **1991**, *113*, 862.

transfer would be highly exothermic for some of the reagents studied but was not observed. Proton transfer dominates the chemistry of most known distonic radical cations.^{1-4,11,12} However, deprotonation does not occur readily for the distonic phosphonium ion studied here although deprotonation through 1,2-elimination would be exothermic by 9 kcal/mol for the triethylamine base, and exothermic 1,2-eliminations are often fast in the gas phase.¹⁶ It should be noted here that the limited amount of data available on *even-electron* phosphonium ion suggests that these ions are also quite unreactive in the gas phase. For example, it was observed during this study that methylated trimethyl phosphite, $(CH_3O)_4P^+$, does not react with trimethyl phosphite (Scheme V) in spite of the fact that methyl cation transfer from the ion to trimethyl phosphite is expected to be exothermic by 10 kcal/mol.¹⁷

The results presented here demonstrate that gaseous ions with spatially separated radical and charge sites can be quite unreactive in the gas phase. Thus far, high reactivity has only been observed^{1-4,11,14} for those distonic ions that are Brønsted acids: these ions undergo fast deprotonation if the reaction is exothermic. It is concluded that a *spatially separated radical and charge site does not necessarily lead to high reactivity in gaseous radical cations*, and that *high reactivity may not be a general characteristic of distonic radical ions*.

Acknowledgment. Acknowledgment is made to the donors of the Petroleum Research Fund, administered by the American Chemical Society, and to the National Science Foundation (Grant CHE-9107121), for partial support of this research.

(16) See, for example: Occhiucci, G.; Speranza, M.; de Koning, L. J.; Nibbering, M. M. *J. Am. Chem. Soc.* **1989**, *111*, 7387.

(17) McMahon, T. B.; Heinis, T.; Nicol, G.; Hovey, J. K.; Kebarle, P. J. *Am. Chem. Soc.* **1988**, *110*, 7591.

The Surface Chemistry of Vinyl Iodide on Pt(111)

Z.-M. Liu, X.-L. Zhou, D. A. Buchanan, J. Kiss, and J. M. White*

Contribution from the Department of Chemistry and Biochemistry, University of Texas at Austin, Austin, Texas 78712. Received July 29, 1991

Abstract: Regardless of exposure, only submonolayer amounts of vinyl iodide (CH_2CHI) decompose, either during adsorption on Pt(111) at 100 K or during subsequent heating to 165 K. The remainder desorbs molecularly. The dissociation products are vinyl (CH_2CH) fragments, an important C_2 intermediate in hydrocarbon catalysis, and atomic iodine. Using the tools of surface science we have explored the formation and subsequent reactions of vinyl species in the presence of unavoidably coadsorbed atomic iodine. While some vinyl exists up to 450 K, there are two important and competitive lower temperature reaction channels which lead to ethylidyne (CCH_3) and ethylene (CH_2CH_2). From our results, we conclude that the rate of ethylidyne formation from adsorbed ethylene is controlled by the rate at which the first C-H bond in ethylene breaks, and in agreement with Zaera,^{1,2} we find that vinyl is a facile intermediate in the process.

1. Introduction

Numerous experimental and theoretical studies have dealt with the chemisorption and reactions, particularly to form ethylidyne, of ethylene on Pt(111).³⁻⁵ During heating from low temperatures, a strong hydrogen-desorption peak, which accompanies the de-

composition of di- σ -bonded ethylene to form ethylidyne, is observed near 300 K. A second strong hydrogen-desorption peak, at 512 K, accompanies the conversion of ethylidyne to a polymeric hydrogen-deficient species.⁴ Although the structures of ethylene and ethylidyne on Pt(111) have been well established, the mechanism of conversion from ethylene to ethylidyne remains controversial. Several intermediates, such as ethyl (CH_2CH_3),⁶ vinyl ($CHC-H_2$),^{1,2} ethylidene ($CHCH_3$),⁷ and vinylidene (CCH_2),⁸ have been

(1) Zaera, F. *J. Am. Chem. Soc.* **1982**, *111*(12), 4240.

(2) Zaera, F. *Surf. Sci.* **1989**, *219*, 453.

(3) Lloyd, K. G.; Campion, A.; White, J. M. *Catal. Lett.* **1989**, *2*, 105 and references therein.

(4) Carter, E. A.; Koel, B. E. *Surf. Sci.* **1990**, *226*, 339 and references therein.

(5) Silvestre, J.; Hoffmann, R. *Langmuir* **1985**, *1*(6), 621.

(6) Bent, B. E. Ph.D. Dissertation, University of California—Berkeley, 1986.

(7) Ibach, H.; Lehwald, S. *J. Vac. Sci. Technol.* **1978**, *15*, 407.

(8) Baro, A. M.; Ibach, H. *Vide, Couches Minces, Suppl.* **1980**, *201*, 458.

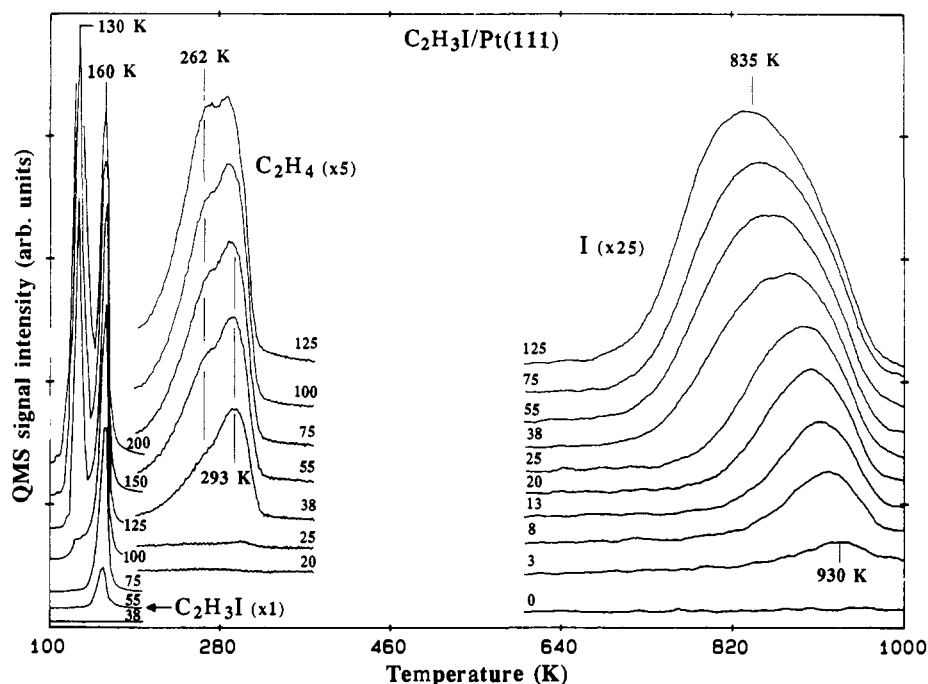


Figure 1. TPD spectra of mass 27 ($C_2H_3^+$), 127 (I^+), and 154 ($C_2H_3I^+$) for various C_2H_3I exposures (indicated by the dosing time on each curve). The exposure temperature was 100 K, and the TPD heating rate was 6 K/s.

proposed. In deuterium-substitution experiments, Zaera^{1,2} proposed that the formation of vinyl fragments, instead of ethylidene, should be favored in the conversion mechanism mentioned above.

In order to confirm that vinyl species play an important role, we studied the adsorption, dissociation, and reactions of vinyl iodide on Pt(111) using a variety of surface science tools. Because the C-I bond is much weaker than the C-H bond, we expect that C_2H_3I dissociates to form $CHCH_2$ fragments at lower temperatures than does C_2H_4 . Indeed, we found that, even at 100 K, vinyl fragments form. They readily convert directly to ethylidyne at temperatures as low as 120 K. Hydrogenation of $CHCH_2$ to ethylene and ethyl is also observed, but only for coverages above a threshold and/or in the presence of coadsorbed atomic hydrogen.

2. Experimental Section

The experiments were carried out in two separate ultrahigh-vacuum chambers. One was equipped with temperature-programmed desorption (TPD), temperature-programmed secondary-ion mass spectrometry (TPSIMS), high-resolution electron energy loss spectroscopy (HREELS), and Auger electron spectroscopy (AES) facilities and has been described elsewhere.⁹ The second chamber housed a Kratos Series 800 X-ray photoelectron spectrometer (XPS) and TPD equipment; a more detailed description has been given previously.¹⁰

The Pt(111) crystal was cleaned by Ar ion sputtering, oxidation at 900–1000 K in 5×10^{-8} Torr of oxygen to remove carbon, and annealing at 1200 K for several minutes to remove residual oxygen. The surface cleanliness was checked by AES. Vinyl iodide (99%, Pfaltz & Bauer) was purified by several freeze-pump-thaw cycles under liquid nitrogen. The vinyl iodide was dosed through a 3-mm-diameter tube that terminated approximately 1 cm from the sample.

TPD and TPSIMS were performed with a temperature ramping rate of 6 or 4.5 K/s. The temperature was measured with a chromel–alumel thermocouple spot-welded to the back of the sample. An 800-eV Ar^+ beam and a beam flux of 5–30 nA/cm² was used for TPSIMS. The dosing temperature was 100 K unless otherwise noted.

In XPS measurements, a Mg K α source was used and the analyzer was set for 40-eV pass energy and 0.05- or 0.10-eV step size. XPS core level spectra of I(3d_{5/2}) and C(1s) were recorded.

HREELS measurements were carried out with a primary beam energy of 6.1 ± 0.2 eV and a resolution of 10–12 mV full width at half-maximum (FWHM). In the annealing sets described below, the sample was

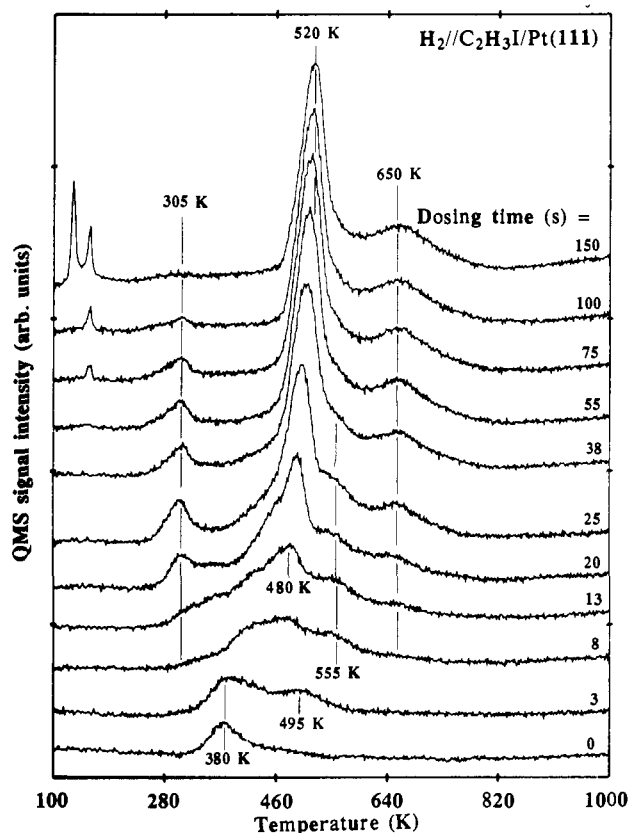


Figure 2. TPD spectra of mass 2 (H_2^+) for various C_2H_3I exposures (indicated by the dosing time on each curve). The exposure temperature was 100 K, and the heating rate was 6 K/s.

flushed to the desired temperature and cooled to 105 K before the spectra were taken.

3. Results

3.1. C_2H_3I /Pt(111). **3.1.1. TPD and AES.** Detailed TPD spectra are presented in Figures 1 and 2; peak areas and the AES C/Pt ratio as a function of dosing time are summarized in Figure 3. Briefly, TPD and AES demonstrate the following. The only

(9) Mitchell, G. E.; Radloff, P. L.; Greenleaf, C. M.; Henderson, M. A.; White, J. M. *Surf. Sci.* **1987**, *183*, 403.

(10) Jo, S. J.; Zhu, X.-Y.; Lennon, D.; White, J. M. *Surf. Sci.* **1991**, *241*, 231.

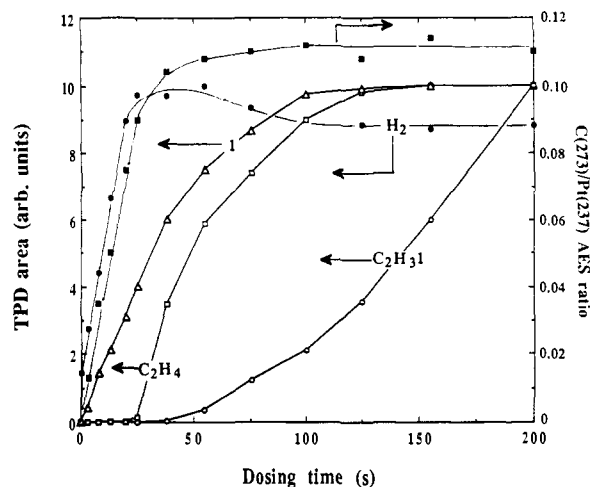


Figure 3. Exposure time dependence of TPD areas, from Figures 1 and 2, for H_2 , C_2H_4 , I, and C_2H_3I , and of the $C(273)/Pt(237)$ AES ratio.

products desorbing up to 1000 K are parent C_2H_3I , H_2 , C_2H_4 , and atomic I. After TPD, there is a significant C AES signal.

Figure 1 shows TPD spectra of C_2H_3I , C_2H_4 , and I as a function of dosing time (designated on each curve). Indicating complete C-I dissociation, no molecular C_2H_3I desorbs for doses shorter than 38 s (Figure 3). For longer doses, a parent peak appears at 160 K and, with no shift, intensifies to saturation (near 110 s). An unsaturable peak then appears at 130 K. We assign the 130 K peak to the physisorbed multilayers and the 160 K peak to the chemisorbed monolayer C_2H_3I . For doses shorter than 38 s, the atomic I TPD area increases linearly with time, and for doses longer than 125 s, the parent TPD area increases linearly. Both indicate a constant sticking coefficient. This fact is used in the quantitative coverage estimates that follow.

Surface I, derived from C-I dissociation, desorbs atomically above 700 K. Its peak temperature shifts downward with increasing dose (from 930 K for 3 s to 835 K for 125 s), and the TPD area saturates (Figure 3) for doses exceeding 100 s. I^+ signals are also found at 130 and 160 K (not shown), but they are the quadrupole mass spectrometer (QMS) ionizer cracking fragments of parent C_2H_3I . In agreement with Zaera,² who studied C_2H_3I on Pt(111), we find that I is lost from the surface around 800 K. Our interpretation, atomic desorption, is different. On the basis of XPS signal loss but the lack of a QMS signal for I, Zerra² suggested, we believe erroneously, that diffusion into Pt might be important.

Ethylene (C_2H_4) desorption occurs, but only for doses longer than 25 s. Like I and the chemisorbed parent, its peak area (Figure 3) saturates at 110 s. The desorption begins at ~200 K, nearly 50 K lower than for directly dosed ethylene,¹¹ and two peaks are apparent with increasing exposure (293 and 262 K). The desorption of molecular ethylene implies a surface reaction (most likely the hydrogenation of vinyl species), described in detail below. The absence of ethylene TPD for low doses indicates competing reaction channels and important coverage dependences (site blocking and stabilization of key intermediates).

Figure 2 shows TPD spectra of H_2 ($m/e = 2$). We use the nomenclature Z//Y/X/Pt(111) to indicate TPD of Z from Pt(111) dosed first with X and then with Y. Without dosing C_2H_3I , there is a small peak at 380 K due to the adsorption of background H_2 . For low exposures (3 and 8 s), TPD shows multiple, coverage-dependent H_2 peaks above 300 and below 600 K. These are ascribed to two sources: background H_2 and decomposition of C_2H_3I . For intermediate exposures (13–25 s), there are four H_2 peaks; three of them, 305, 555, and 650 K, are independent of C_2H_3I exposure, while the fourth peak shifts, for 13–25 s, from 480 to 510 K. For higher exposures, the peak positions do not change, the 555 K peak is overwhelmed by the 520 K peak, and

the 305 K peak rises and then decays. The low-temperature signals for exposures greater than 55 s are cracking fragments of parent vinyl iodide desorption.

The four higher temperature peaks are reminiscent of H_2 desorption following ethylene adsorption on Pt(111),¹¹ a particularly relevant case since ethylene desorbs here (Figure 1). Following the ethylene case, these peaks can be assigned as follows:¹¹ (1) the 305 K peak to atomic H recombination occurring as the result of C-H bond cleavage in di- σ -bonded ethylene, the latter formed at slightly lower temperatures by hydrogenation of vinyl; (2) the 520 K peak to one or more C-H bond cleavages in ethylidyne; and (3) the 650 K peak to C-H bond cleavage in the remaining surface C_xH_y polymer. Referring to Figure 3, the H_2 TPD area increases linearly up to 25 s. Linearity is expected since H_2 is the only H-containing TPD product and, by extrapolation, the sticking coefficient is constant. After a plateau from 25 to 55 s, the H_2 TPD area decreases slightly and becomes constant for doses longer than 110 s.

In addition to TPD areas, Figure 3 shows the $C(273)/Pt(237)$ AES ratio measured after TPD to 1000 K. It increases sharply to saturation at 110 s, consistent with the behavior of C_2H_3I , H_2 , C_2H_4 , and I TPD areas. It is evident that C-I dissociation ceases upon completion of the first monolayer and perhaps even before. For the chemisorbed layer, however, both molecular desorption and dissociation occur, with dissociation dominating at low coverages.

With reasonable assumptions, we can estimate some relevant coverages. Assuming, for dissociative H_2 adsorption on Pt(111) at 100 K, that saturation is reached when the H/Pt surface atom ratio reaches unity,¹² we can calibrate H_2 desorption peak areas. On the basis of the measured saturation H_2 TPD area, we calculate that the initial linear increase in H_2 TPD area (Figure 3) implies a C_2H_3I adsorption rate of 0.004 adsorbates, where no ethylene desorbs, per surface Pt atom per second (0.004 ML/s (monolayer/second)). Because the completion of the first layer C_2H_3I requires 110 s, the saturation first layer coverage, were there no dissociation, would be 0.44 ML assuming, consistent with the multilayer growth rate, a coverage-independent sticking coefficient. In fact, there is dissociation, and of the 0.44 ML that sticks, we conclude that 0.14 ML (~30%) desorbs molecularly and 0.30 ML (~70%) dissociates. We can go further using the low-coverage H_2 TPD data (complete dissociation) to calibrate the C/Pt AES data. Of the 0.30 ML that dissociates, only 0.13 ML decomposes completely to surface carbon. Thus, for a saturated chemisorbed monolayer of C_2H_3I on Pt(111) at 100 K (0.44 ML), the C_2H_4 yield is 0.17 ML (40%). For these coverage conditions, the H_2 TPD area indicates an ethylidyne coverage of 0.10 ML.

To establish more clearly the connections between ethylene and vinyl iodide surface chemistry, we show in Figure 4 dihydrogen TPD spectra for saturation monolayer doses of C_2H_3I , C_2H_4 , and C_2D_4 . In excellent agreement with earlier work,^{11,13,14} there are discernible peaks for C_2H_4 at 302, 502, and 645 K and shoulders below and above 645 K. A small isotope effect, but nothing more, distinguishes the C_2D_4 case. For ethylene, it is well established that the lowest dihydrogen TPD peak is reaction-limited C-H bond cleavage in di- σ -bonded ethylene, a dissociation accompanied by ethylidyne formation.¹¹ For C_2H_3I in Figure 4, this peak is absent, indicating that the reaction channel converting di- σ -bonded ethylene to ethylidyne is not operative. This channel (305 K) rises and falls as a function of vinyl iodide exposure (Figure 2).

The higher temperature regions for all three cases are strikingly similar, supporting the notion that ethylidyne formation and decomposition contribute to the surface chemistry of vinyl iodide. There are, however, reproducible differences; for vinyl iodide, the lower temperature peak is shifted to higher temperatures (502 to 520 K) and the shoulders observed for both ethylenes are absent. To pursue this further, we prepared deuterated ethylidyne, CCD_3 , by dosing a saturation amount of C_2D_4 at 100 K and heating it

(12) Weinberg, W. H. *Surv. Prog. Chem.* **1983**, *10*, 1.

(13) Steininger, H.; Ibach, H.; Lehwald, S. *Surf. Sci.* **1982**, *117*, 341.

(14) Salmeron, M.; Somorjai, G. A. *J. Phys. Chem.* **1982**, *86*, 341.

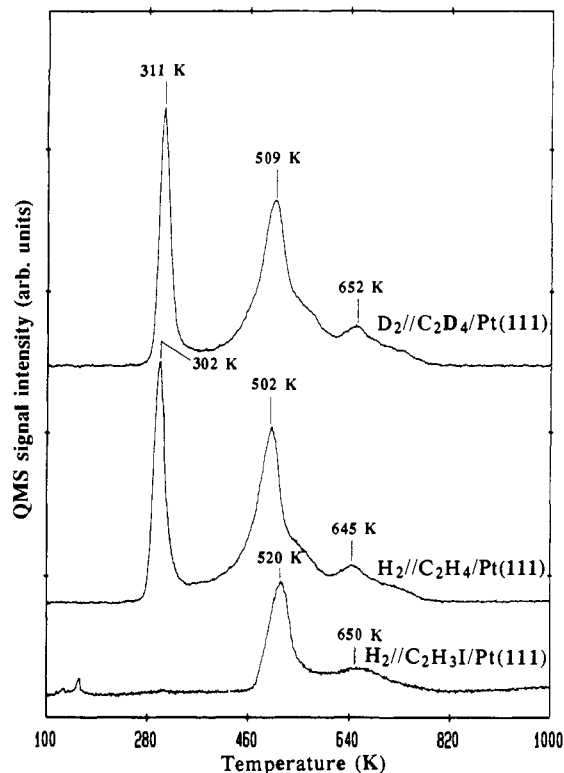


Figure 4. TPD spectra of dihydrogen for saturated monolayer C_2H_3I , C_2H_4 , and C_2D_4 . The exposure temperature was 100 K, and the heating rate was 6 K/s.

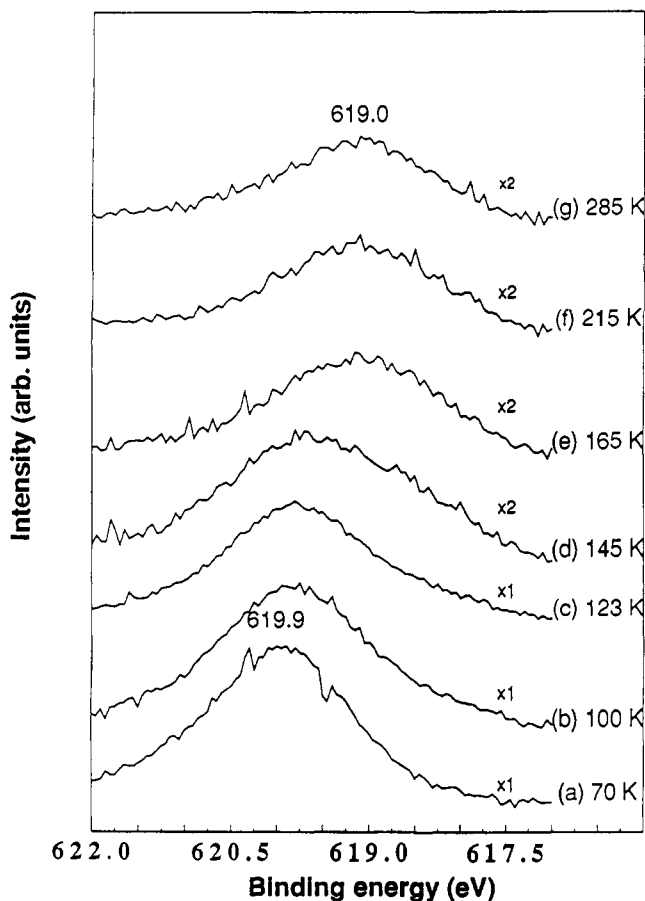


Figure 5. I(3d) XPS core level spectra for a multilayer dose of C_2H_3I at 70 K (a), then warmed briefly to (b) 100 K, (c) 123 K, (d) 145 K, (e) 165 K, (f) 215 K, and (g) 285 K. All XPS spectra were taken after recoiling to below 100 K.

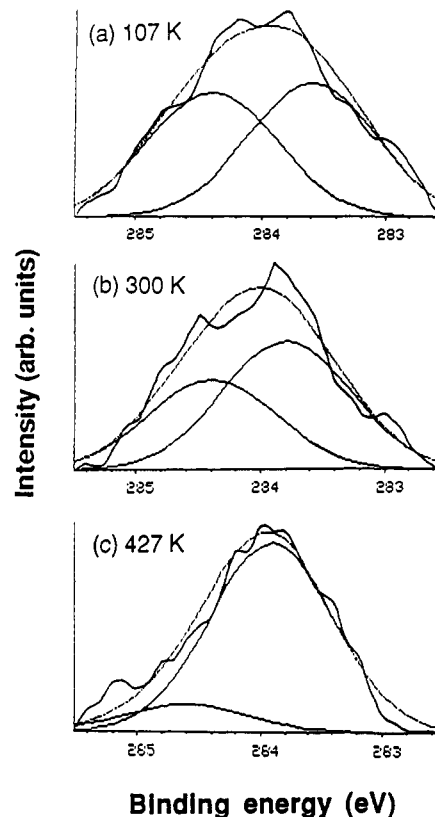


Figure 6. C(1s) XPS core level spectra for a multilayer dose of C_2H_3I on Pt(111) at 70 K, then warmed briefly to (a) 107 K, (b) 300 K, and (c) 427 K. All spectra were taken after recoiling to below 100 K. The broad, somewhat noisy spectra are the experimental data, while the smooth curves are synthesized fits using Gaussian profiles.

to 375 K. After recoiling to 100 K, we added 0.44 ML of C_2H_3I . During subsequent TPD, there was significant dissociation, and the resulting profile mimicked the lower curve of Figure 4, i.e., shifted TPD with no shoulders. This experiment indicates a discernible role for I, i.e., stabilizing ethylidyne, thereby shifting its reaction-limited decomposition to slightly higher temperatures, and causing TPD peaks to sharpen.

3.1.2. XPS. X-ray photoelectron spectroscopy, undertaken to provide direct evidence for changes in surface atomic composition and chemical environment, is summarized in Figures 5 and 6. I(3d) for a multilayer of C_2H_3I on Pt(111), dosed at 70 K, has a peak at 619.9 eV. While heating to 100 K desorbs nothing, the I(3d) peak broadens slightly toward lower binding energy (BE), signaling some C-I bond dissociation. With further heating, the peak becomes less intense, broadens further, and shifts to 619.0 eV at 165 K. The intensity loss (note the scale change at 145 K) is due to the desorption of C_2H_3I multilayers at 130 K. The shift to lower BE is attributed to thermally activated C-I dissociation. These changes cease above 165 K, indicating that parent molecules which undergo dissociation do so below 165 K. Taking the area of curve d (145 K) as one monolayer (see Figure 1), we calculate, on the basis of the area at 215 K, that 72% of C_2H_3I in the first monolayer is dissociated. This compares favorably with the estimate (70%) from TPD results (see above).

Figure 6 shows C(1s) spectra for a multilayer dosed on Pt(111) at 70 K and then heated to the indicated temperatures. The thick, somewhat noisy curves are the experimental data; the smooth curves are synthesized fits using Gaussian profiles with widths based on standard C(1s) spectra.^{15,16} At 107 K, as expected, the width requires two peaks (283.6 and 284.4 eV) of nearly equal intensity in the fit. These are assigned to the two C(1s) chemical

(15) Akhter, S.; Allan, K.; Buchanan, D.; Cook, J. A.; Campion, A.; White, J. M. *Appl. Surf. Sci.* **1988-1989**, *35*, 241.

(16) Freyer, N.; Pirug, G.; Bonzel, H. P. *Surf. Sci.* **1983**, *126*, 487.

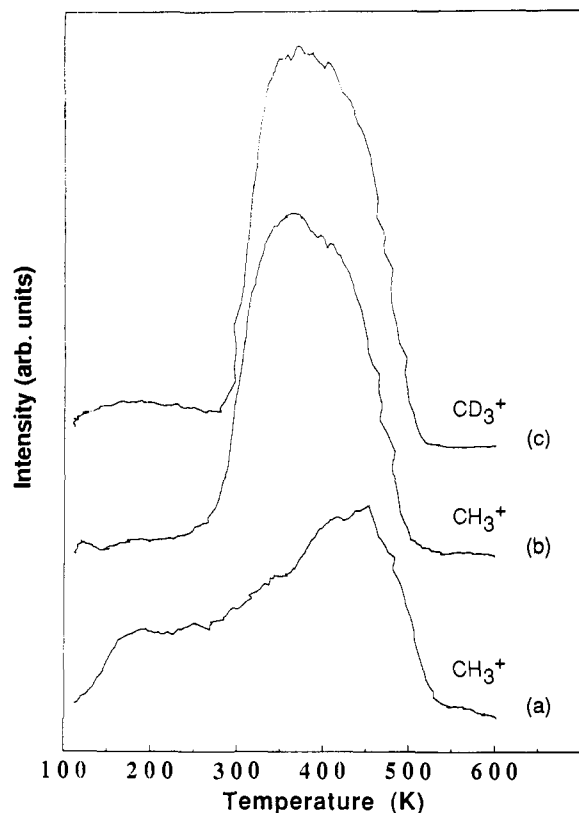


Figure 7. TPSIMS spectra of methyl ions from surfaces saturated with monolayers of C_2H_3I (a), C_2H_4 (b), and C_2D_4 (c). The dosing temperature was 120 K, and the heating rate was 6 K/s.

environments in adsorbed molecular C_2H_3I , with the higher BE associated with the I environment. They compare very favorably with results for undissociated vinyl chloride on Pt(111) (283.4 and 284.6 eV).¹⁶ Some dissociation can account for the slightly more intense lower BE peak. At 300 K, where a significant amount of ethylidyne forms, the lower BE region (283.8 eV) intensifies, its ratio to the higher BE peak becoming 1.5. This continues to 427 K, where the ratio is 10. These BEs cannot be unambiguously assigned to a single species, but, considering the TPD and TPSIMS (see TPSIMS below) results, there is a good correlation between the intensity of the higher BE peak and vinyl concentration. Vinyl is presumably surrounded by atomic iodine and, thus, shifted to a higher BE (284.4 eV) than might otherwise be expected.

3.1.3. TPSIMS. Previous work¹¹ shows that the CH_3^+ TPSIMS signal ($m/e = 15$) can be used to monitor the surface concentration of ethylidyne. Figure 7 summarizes methyl ion signals after dosing C_2H_3I , C_2H_4 , and C_2D_4 ; the analogous TPD spectra are shown in Figure 4. For C_2H_4 and C_2D_4 , the CH_3^+ and CD_3^+ signals begin to increase (ethylidyne formation) above 250 K and decrease (ethylidyne decomposition) above 400 K, in agreement with the earlier work.¹¹ There is a small isotope effect that favors the formation and decomposition of CCH_3 , consistent with the TPD results. For C_2H_3I , however, the CH_3^+ signal begins to increase at temperatures as low as 120 K. After a plateau from 200 to 300 K, it increases again until it starts to decay above 450 K. In none of the three cases is there a CH_3^+ signal above 550 K. The CH_3^+ signal from C_2H_3I is of particular interest; its high-temperature behavior tracks the decomposition of ethylidyne, just as it does for the ethylenes. We take the low-temperature growth as evidence for facile vinyl conversion to ethylidyne without intervention of hydrogenation to ethylene. The increase between 300 and 450 K is taken to reflect ethylidyne formation from vinyl, stabilized in the presence of high coverages of coadsorbed species (see HREELS below).

3.1.4. HREELS. The evidence shown above points to the dissociation of vinyl iodide and to the formation of at least three

Table I. Assignments for Vinyl Iodide and Vinyl

	$C_2H_3I^a$	$C_2H_3/Ni(100)^b$	$C_2H_3I/Pt(111)^c$	$C_2H_3/Pt(111)^c$
$\nu-XC$	535		555	
ρ_w-CH_2	990	915	955	955
ρ_w-CH	946	760	nr ^d	690
ρ_r-CH_2				
ρ_r-CH_2	909	1160	nr	nr
$\delta-CH$	1229	1280	1255	1255
$\delta-CH_2(s)$	1376	1405	1380	1380
$\nu-C=C$	1593	1555	1565	1600
$\nu-CH$	3060	2920	3070	2920
$\nu-CH_2(s)$	3000	2920	nr	2920
$\nu-CH_2(as)$	3110	3090	3070	nr

^aReference 28. ^bReference 17. ^cThis work. ^dNot resolved.

Table II. Assignments for Di- σ -Bonded Ethylene

	$C_2H_4/Pt(111)^a$	$C_2H_4/Cl/Pt(111)^b$	$C_2H_4/I/Pt(111)^c$
$\nu-PtC$	470	457	470
ρ_w-CH_2	980	985	nr ^d
$\nu-CC$	1050	1055	nr
$\delta-CH_2(s)$	1430	1433	1410
$\nu-CH_2(s)$	2920	2973	2970
$\nu-CH_2(as)$	3000	nr	nr

^aReference 13. ^bReference 3. ^cThis work. ^dNot resolved.

Table III. Assignments for Ethylidyne

	$CCH_3/Pt(111)^a$	$CCH_3/Cl/Pt(111)^b$	$CCH_3/I/Pt(111)^c$
$\nu-PtC$	430	433	440
ρ_r-CH_3	980	920	nr ^d
$\nu-CC$	1130	1125	1125
$\delta-CH_3$	1350	1352	1360
$\nu-CH_3(s)$	2890	nr	nr
$\nu-CH_3(as)$	2950	2970	2940

^aReference 13. ^bReference 3. ^cThis work. ^dNot resolved.

surface species, vinyl ($CHCH_2$), ethylene (C_2H_4), and ethylidyne (CCH_3). The application of HREELS provides deeper insight into the nature of these surface processes.

Figure 8 shows HREELS spectra as a function of C_2H_3I exposure on Pt(111) at 105 K (exposures in dosing time are indicated on each curve). The vibrational assignments for vinyl iodide and vinyl are given in Table I. For a 25-s dose, the observed losses at 690, 955, 1380, 1600, and 2920 cm^{-1} are characteristic of surface vinyl species.¹⁷ The absence of the C-I stretch (555 cm^{-1}) indicates that all the C-I bonds dissociate at 105 K, supporting the XPS results. The shoulder at 1125 cm^{-1} may reflect some ethylidyne, even at this temperature. For a 50-s dose, both the C-I stretching mode at 555 cm^{-1} and a C-H shoulder at 3070 cm^{-1} appear, substantiating the presence of molecular C_2H_3I . For doses above 100 s, there are additional losses at 1255 cm^{-1} (CH rocking) and 1910 cm^{-1} (overtone of 955 cm^{-1}). The peak shifts (upward for 2920 cm^{-1} and downward for 1600 cm^{-1}) are consistent with the dominance of molecular vinyl iodide, rather than dissociated vinyl, at high coverages.

Figure 9 shows HREELS spectra as a function of annealing temperature for a multilayer dose of C_2H_3I on Pt(111) at 105 K (the annealing temperatures are indicated on each curve, and spectra were taken after recoiling). The vibrational assignments for ethylene and ethylidyne are given in Tables II and III, respectively. After the surface is heated to 145 K (not shown), all the features associated with molecular C_2H_3I decrease, reflecting multilayer desorption. The signal at 555 cm^{-1} (C-I stretch) indicates the presence of intact chemisorbed parent molecules. The peak at 3070 cm^{-1} shifts to 3000 cm^{-1} and becomes broader, suggesting the coexistence of $CHCH_2$ and C_2H_3I . After annealing to 180 K, the 555- cm^{-1} loss disappears, indicating the absence

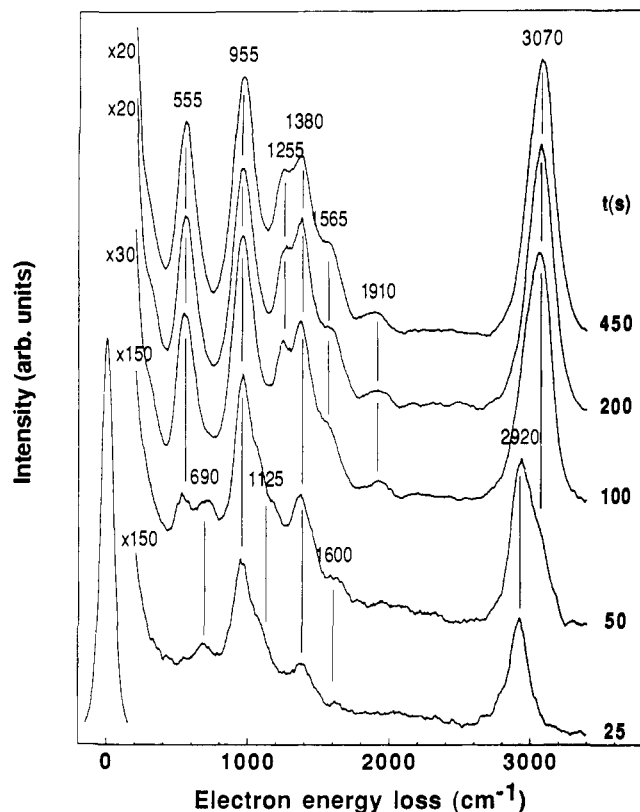


Figure 8. HREELS spectra as a function of C_2H_3I exposure (exposures in dosing time are indicated on each curve) on Pt(111) at 105 K.

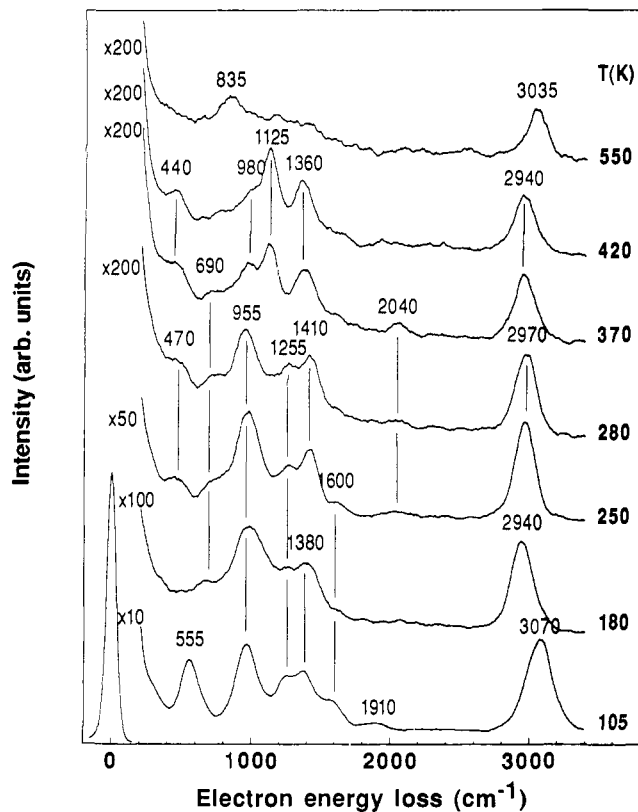


Figure 9. HREELS spectra for a multilayer dose of C_2H_3I on Pt(111) at 105 K (bottom spectrum) and warmed briefly to various temperatures as indicated.

of C-I bonds. This is consistent with the XPS data. According to TPD, monolayer C_2H_3I has desorbed. Shifts (3000 to 2940 cm^{-1} and 1565 to 1600 cm^{-1}) provide additional evidence for the conversion of molecular C_2H_3I to $CHCH_2$. The emergence of

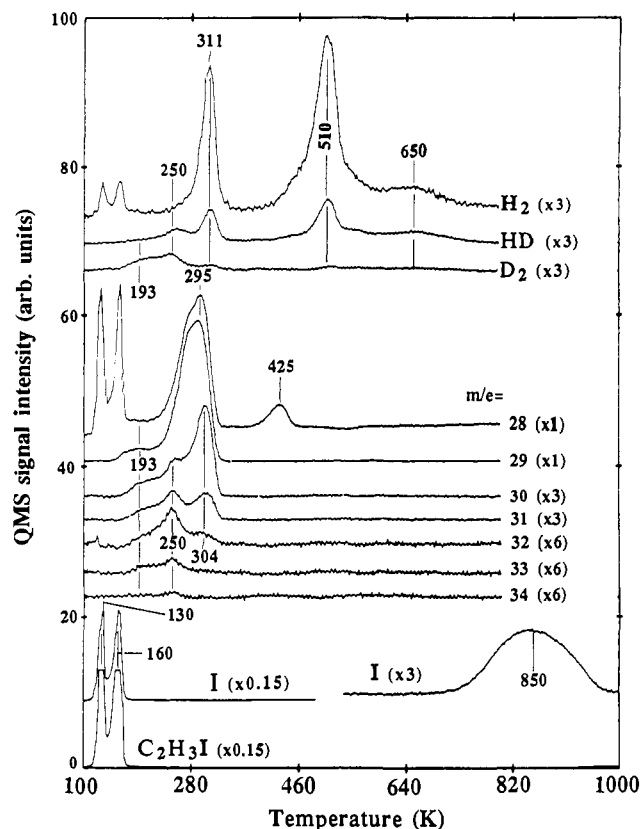


Figure 10. TPD spectra taken after coadsorbing 0.18 ML D and multilayer C_2H_3I on Pt(111) at 100 K. Heating rate was 6 K/s.

a CH wagging mode at 690 cm^{-1} also supports the formation of $CHCH_2$ fragments. We believe that $CHCH_2$ fragments dominate at this temperature (180 K), but there may be small amounts of CCH_3 or C_2H_4 as well.

New features appear when the surface is heated from 180 to 250 or 280 K, signaling ethylene formation (Table II). First, there is a C-Pt mode at 470 cm^{-1} , and further, the peaks at 1380 and 2940 cm^{-1} shift to 1410 and 2970 cm^{-1} , respectively. Above 300 K, the losses due to CCH_3 (Table III) dominate the spectra, i.e., 440 cm^{-1} for Pt-C stretching, 1125 cm^{-1} for C-C stretching, 1360 cm^{-1} for CH_3 symmetric bending, and 2940 cm^{-1} for CH_3 symmetric and asymmetric stretching. It is noteworthy that there is some evidence for residual $CHCH_2$; the CH_2 wagging mode shifts from 955 cm^{-1} to 980 cm^{-1} and persists to 420 K, consistent with the proposed high-temperature conversion of vinyl to ethynyl noted in TPSIMS. Other vinyl losses are presumed unobservable due to low intensity and overlapping. After annealing to 550 K, all the ethynyl and vinyl features are absent; there are losses at 835 and 3035 cm^{-1} which correspond to CH bending and stretching modes¹⁸ and unresolved intensity throughout the 1000–1600- cm^{-1} region.

3.2. $C_2H_3I/D/Pt(111)$. 3.2.1. TPD. Because of the insight often provided by isotope labeling, we undertook coadsorption studies in which two coverages (0.18 and 0.47 ML) of preadsorbed D were covered with slightly more than 1 ML of vinyl iodide at 100 K. In TPD, we observed hydrogenation and H-D exchange products, i.e., D-labeled ethylene and ethane.

Figures 10 and 11 summarize the TPD results for these two cases (m/e labels on each curve). Compared to vinyl iodide dosed alone (Figures 1 and 2), the presence of 0.18 ML of D causes the following: (1) It slightly lowers the amount of vinyl iodide decomposed (the I desorption is 90% of its original value). (2) It leads to facile conversion of vinyl to ethylene (the ethylene desorbs at 295 K, and the dihydrogen desorption at 311 K marks ethylene-to-ethynyl conversion). (3) It leads to ethane, which

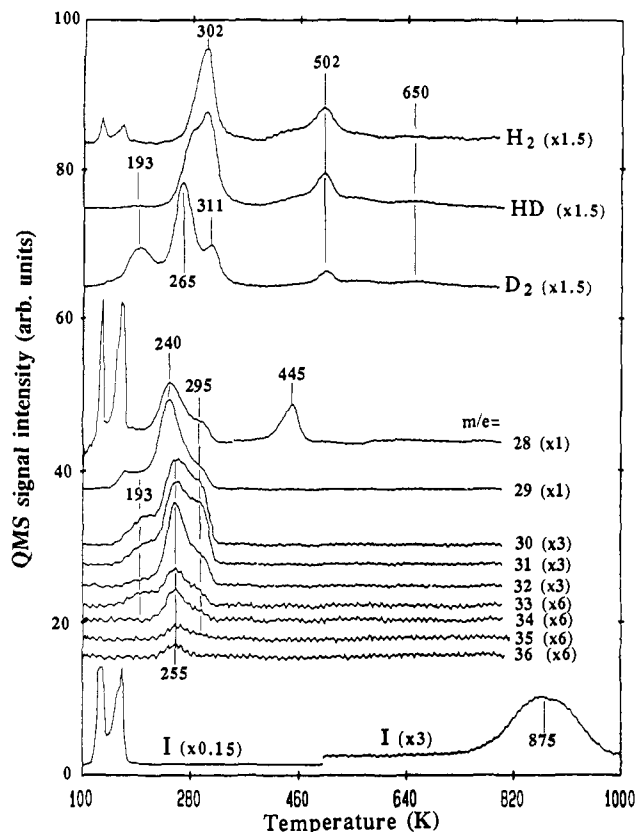


Figure 11. TPD spectra taken after coadsorbing 0.47 ML D and multilayer C_2H_3I on Pt(111) at 100 K. Heating rate was 6 K/s.

forms and desorbs at 250 K (30–34 amu). (4) It shifts some dihydrogen desorption to 250 K and, for D_2 , to 193 K. Note that the 425 K peak in Figure 10 is caused by background CO. This case is consistent with the hydrogenation of vinyl to ethylene.

Raising the D coverage has a significant impact. Compared to the 0.18-ML case (Figure 10), the presence of 0.47 ML of D has the following effects (Figure 11): (1) It suppresses vinyl iodide decomposition (the I desorption is 70% of its former value). (2) It increases the amount of ethane formed, which also has a higher D content (perdeuterated ethane is observed at 36 amu, and the 32-amu signal is 5-fold larger). (3) It strongly enhances the amount of dihydrogen desorbed in the 300 K region. As discussed below, this case is consistent with hydrogenation of vinyl to ethyl at or below 200 K.

Returning to Figure 10, we note two peaks at 130 K (multilayer) and 160 K (monolayer) for molecular vinyl iodide desorption, just as in the absence of D. The area of the 310 K dihydrogen peak is $\sim 25\%$ of the total area of the 310, 510, and 650 K peaks, confirming that, in this case, ethylidyne is formed exclusively from ethylene and not directly from vinyl. For each of the three peak temperatures, the peak areas for the three isotopes have the same ratios (23% D), reflecting the facts that all of the D is incorporated below 300 K and isotope effects play a negligible role in the decomposition of ethylidyne and its C_2H_3 products. We conclude that, on average, each ethylene contains one D atom.

Dealing with the weak C_2 hydrocarbon signals first, we note that m/e values up to 34, but not higher, are detected. At 250 K for $m/e = 30-34$, there are peaks which are assigned to ethanes containing up to four D atoms and attributed to self-hydrogenation of ethyl intermediates, based on other work involving ethyl fragments derived from the thermal dissociation of $C_2H_5I^2$ and photodissociation of C_2H_5Cl .¹⁹ The C_2 peak at 304 K for $m/e = 30-32$ is attributed, as in other work,²⁰ to ethane derived from

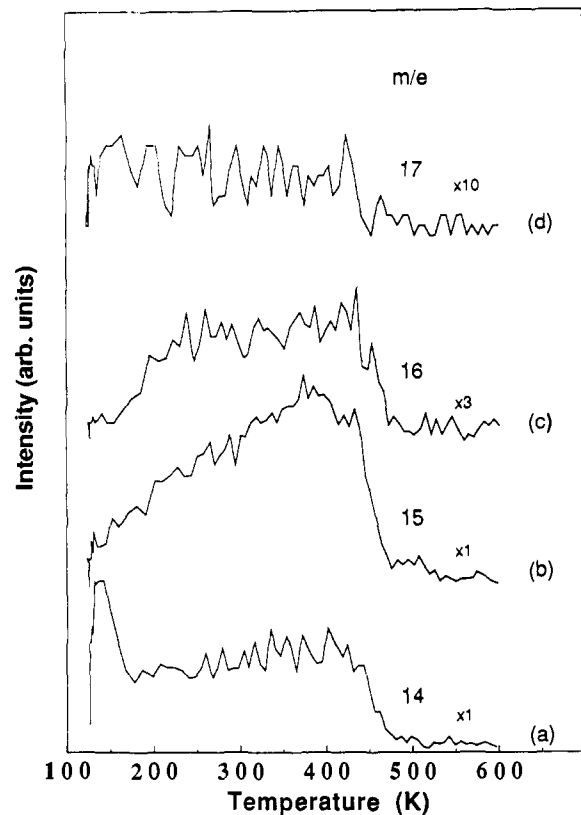


Figure 12. TPSIMS spectra for positive ions after coadsorbing 0.47 ML D and multilayer C_2H_3I on Pt(111) at 120 K. The ion masses are (a) 14 (CH_2), (b) 15 (CH_3 , CHD), (c) 16 (CH_2D , CD_2), and (d) 17 (CH_2D_2). The heating rate was 4.5 K/s.

the self-hydrogenation of ethylene. The $m/e = 32$ signal at 304 K is assigned to $C_2H_4D_2$; its intensity is low. No $C_2H_3D_3$ is detectable. These low intensities reflect the relatively low concentration of D and, in this temperature region, the rapidly increasing concentration of H as ethylene decomposes to ethylidyne. The small peak at 193 K for $m/e = 30-33$ is coincident with D_2 desorption and is attributed to the facile, but transient, deuteration of vinyl (i.e., $3D(a) + CHCH_2(a) \rightarrow C_2H_3D_3$). At this temperature, we suppose that isotope exchange is not competitive. If it were, we would observe even more incorporation of D.

Turning to the dominant signals (note the scale factors) in the C_2 region, $m/e = 28$ and 29 track each other and show an intense peak at 295 K with a shoulder on the low-temperature side. Comparing fragmentation patterns, we conclude that the $m/e = 28$ signal is mainly due to the cracking of C_2H_3D ($m/e = 29$), a conclusion entirely consistent with the above dihydrogen analysis. While these peaks certainly contain contributions from the fragmentation of the ethane formed at 250 and 304 K, these contributions are negligibly small.

For the most part, a similar analysis is obtained for the higher D coverage. Among the differences, there is isotope labeling that requires exchange. For example, the peaks at 255 K for $m/e = 30-36$ are assigned to ethane with up to six D atoms (36 amu). Hydrogenation without the exchange of $CHCH_2$ would give no more than three D atoms so that, not surprisingly,²¹⁻²³ isotope exchange is competitive here. The signal for $m/e = 35$ is exclusively C_2HD_5 , again indicating isotope exchange. The ethylene self-hydrogenation peaks (295 K) contain up to five D atoms (C_2HD_5 is seen), whereas no more than two D atoms were found for 0.18 ML D. There are additional peaks at 240 K for $m/e = 28$ and 29; these are attributed to C_2H_3D ($m/e = 29$) and its fragment at $m/e = 28$, a product of direct deuteration of C_2H_3 .

(19) Lloyd, K. G.; Roop, B.; Campion, A.; White, J. M. *Surf. Sci.* **1989**, *214*, 227.

(20) Zaera, F. *J. Phys. Chem.* **1990**, *94*, 5090.

(21) Zaera, F. *J. Phys. Chem.* **1990**, *94*, 8350.

(22) Creighton, J. R.; Ogle, K. M.; White, J. M. *Surf. Sci.* **1984**, *138*, L137.

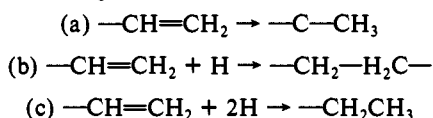
(23) Liu, Z.-M.; Zhou, X.-L.; White, J. M. *Appl. Surf. Sci.* **1991**, *52*, 249.

For the hydrogen isotopes, the spectra are, with one exception, very similar to those observed by Zaera,²¹ who studied $\text{CD}_3\text{CH}_2\text{I}/\text{Pt}(111)$. For example, the peak at 265 K for D_2 and the shoulder near 265 K for H_2 and HD are due to dehydrogenation of ethyl to ethylene. Lower intensity peaks, attributed to the same origin,^{2,19,24} appear at 250 K in Figure 10. Thus, vinyl hydrogenation to ethyl is facile below 250 K in the presence of excess surface atomic hydrogen. The higher temperature peaks are due to the conversion of ethylene to ethylidyne and the decomposition of ethylidyne. In this case, we calculated, as described above, that the H/D ratio in ethylidyne is about 1:1. The 193 K peak for D_2 is an exception and is attributed to the low-temperature recombinative desorption of atomic D under conditions of surface crowding. We conclude that surface ethyl is the dominant intermediate for $\text{C}_2\text{H}_3\text{I}/0.47 \text{ ML D}/\text{Pt}(111)$ and that it facilitates isotope exchange.

3.2.2. TPSIMS. Figure 12 shows TPSIMS spectra of $m/e = 14, 15, 16,$ and 17 (attributable to CH_2, CH_3 and $\text{CHD}; \text{CH}_2\text{D}$ and CD_2 ; and CHD_2 , respectively) following coadsorption of $\sim 0.44 \text{ ML C}_2\text{H}_3\text{I}$ and 0.47 ML D . Only a small low-temperature signal for $m/e = 18$ was observed; this signal and the low-temperature portion of the $m/e = 17$ signal correlate with the desorption of small amounts of background water. There was no evidence for CD_3 formation. In curve a, the peak around 140 K for CH_2 is from parent $\text{C}_2\text{H}_3\text{I}$. Curve b is similar to curve a in Figure 7, but the plateau between 200 and 300 K is not obvious here, for two possible reasons: (1) The formation and decomposition of deuterated ethylene is dominant. (2) The signal-to-noise ratio is not as good. Curve c rises above 150 K, consistent with the TPD of deuterated ethylene. Isotope exchange in ethylidyne formation confirms this notion.

4. Discussion

From the above results and the comparisons made, the following picture emerges, which sheds some light on the mechanism for the conversion of chemisorbed ethylene to ethylidyne on $\text{Pt}(111)$. Partial decomposition, C-I bond cleavage, occurs during adsorption of monolayer $\text{C}_2\text{H}_3\text{I}$ on $\text{Pt}(111)$ at 100 K. During thermal desorption, additional C-I bond cleavage occurs up to the desorption temperature of the chemisorbed parent (160 K). Depending on the coverage of atomic hydrogen, one of three surface reaction channels operates:



The relative importance depends on the surface hydrogen coverages: channel a dominates for hydrogen-deficient surfaces, b dominates for intermediate coverages of atomic hydrogen, and c dominates for high coverages of preadsorbed hydrogen.

The importance of channel a is evidenced by (1) the rise at 120 K of the CH_3^+ signal in TPSIMS, (2) the shoulder at 1125 cm^{-1} in HREELS spectra of low $\text{C}_2\text{H}_3\text{I}$ coverages, (3) the presence of strong ethylidyne vibrational modes above 300 K, and (4) the strong 520 K, but the absence of 300 K, H_2 TPD.

Channel b is evidenced by (1) strong hydrogen desorption at 300 and 520 K, just as found for the conversion of ethylene to ethylidyne, (2) negligible ethylene desorption for low doses of vinyl iodide, (3) steadily increasing amounts of ethylene desorption above a threshold vinyl iodide coverage, and (4) significant ethylene desorption, dominated by $\text{C}_2\text{H}_3\text{D}$, when 20% of a monolayer of D is preadsorbed.

Channel c is evidenced by (1) the desorption of a significant amount of ethane at temperatures known to hydrogenate ethyl fragments and (2) the desorption of ethylene at temperatures where ethyl is known to dehydrogenate.

If ethylene converts to ethylidyne via vinyl, one might question why no vinyl intermediates have been detected when ethylene is dosed on $\text{Pt}(111)$. This is readily explained because the C-H bond

in adsorbed ethylene breaks ($>250 \text{ K}$) at temperatures where vinyl rearrangement to ethylidyne is facile ($<200 \text{ K}$). Unless special circumstances exist, vinyl from ethylene is stabilized; it will never accumulate. On the basis of TPSIMS, XPS, and HREELS, we have found in this study that atomic iodine stabilizes some vinyl, to as high as 450 K. There is some evidence that preadsorbed atomic oxygen may also stabilize some vinyl, because there is an extra CH_3^+ peak at 450 K.¹¹

It is interesting to examine the evidence for isotope exchange. In the presence of preadsorbed D, parent vinyl iodide TPD is unlabeled. Thus, exchange does not occur prior to C-I bond breaking and desorption of the parent. Exchange into the vinyl species occurs, but at low temperatures and high atomic hydrogen concentrations, hydrogenation to ethyl dominates and exchange in the latter is facile.

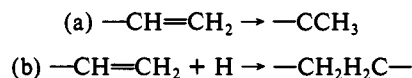
The absence of exchange into the parent suggests that the adsorption geometry of vinyl iodide is similar to that of methyl halides on $\text{Pt}(111)$,²⁵ i.e., bonding through the iodine with the vinyl part pointed into the vacuum. This geometry is consistent with the HREELS data since the intense C=C stretch suggests that the axis through the two carbon atoms should not be parallel to the surface.

When C-I bonds break, the vinyl bonding geometry is not clear. Henderson et al.²⁶ proposed $\eta^2\text{-(C,C) CHCH}_2$ as an intermediate for ethylene decomposition on $\text{Ru}(001)$. Carter and Koel⁴ propose, on the basis of theoretical considerations, a similar fully rehybridized CHCH_2 species as an important ethylene decomposition intermediate. On the basis of these previous experimental and theoretical studies, we cannot rule out the possibility of $\eta^2\text{-(C,C) CHCH}_2$. However, the appearance of the C=C stretching mode at 1600 cm^{-1} up to 250 K suggests that at least part of the surface vinyl retains its C=C double bond. While the η^2 structure may make it easier to account for deuterium exchange, we note that isotope exchange does occur in ethylidyne adsorbed on $\text{Pt}(111)$ ²² and that, in the presence of ethylidyne, ethylene can be hydrogenated to ethane.²⁷

According to theoretical calculations,⁴ the mechanism by which ethylene undergoes $\alpha\text{-H}$ cleavage to form vinyl (the reverse of channel b) and further isomerizes to form ethylidyne cannot be ruled out on the basis of reaction energetics alone. The estimated barrier for $\alpha\text{-H}$ cleavage is fairly large, an expectation confirmed by the isotope effects noted in Figures 4 and 7. This barrier may account for why ethylidyne from ethylene sets in at 310 K, whereas ethylidyne from vinyl occurs below 200 K.

5. Conclusions

Vinyl iodide adsorbs on $\text{Pt}(111)$ at 100 K both molecularly and dissociatively. At high coverages, both the multilayer and monolayer of vinyl iodide desorb at 130 and 160 K, respectively. During heating, additional C-I bond cleavage occurs below the monolayer desorption temperature and, overall, 70% of the vinyl iodide in the first layer dissociates. In the absence of coadsorbed atomic hydrogen, there are two competitive reaction channels for vinyl species:



Vinyl conversion to ethylidyne, reaction a, starts at 120 K, but in the presence of large amounts of I, there is evidence that some vinyl species are stable up to 450 K. Reaction b is enhanced when surface hydrogen is available, as it is when D is preadsorbed or when intermediate coverages of the parent allow for low-temperature C-H cleavage. The desorption of the ethylene from $\text{C}_2\text{H}_3\text{I}$ is reaction-limited and occurs at a lower temperature than

(25) Henderson, M. A.; Mitchell, G. E.; White, J. M. *Surf. Sci.* **1987**, *184*, L325.

(26) Henderson, M. A.; Mitchell, G. E.; White, J. M. *Surf. Sci.* **1988**, *203*, 278.

(27) Godbey, D.; Zaera, F.; Yeates, R.; Somorjai, G. A. *Surf. Sci.* **1986**, *167*, 150.

(28) Torkington, P.; Thompson, H. W. *J. Chem. Soc.* **1944**, *Part I*, 303.

(24) Zaera, F. *J. Am. Chem. Soc.* **1989**, *111*, 8744.

for ethylene chemisorbed alone on Pt(111).

The results suggest that the first C–H bond cleavage is the rate-determining step for ethylidyne formation from ethylene on Pt(111) and that vinyl is a facile intermediate in the conversion of ethylene to ethylidyne.

For high coverages of preadsorbed D, hydrogenation of vinyl to ethyl occurs and leads to TPD product distributions that are consistent with those measured when starting with ethyl iodide.²

Moreover, isotope exchange is facile, leading to some perdeuterioethane desorption.

Acknowledgment. This work was supported in part by the U.S. Department of Energy, Office of Basic Energy Sciences, and by the Exxon Education Foundation.

Registry No. H₂C=CHI, 593-66-8; Pt, 7440-06-4; H₂C=CH₂, 74-85-1; ethylidyne, 67624-57-1; vinyl, 2669-89-8.

Activation of Alkanes by Cr⁺: Unique Reactivity of Ground-State Cr⁺(⁶S) and Thermochemistry of Neutral and Ionic Chromium–Carbon Bonds

Ellen R. Fisher[†] and P. B. Armentrout^{*‡}

Contribution from the Department of Chemistry, University of Utah, Salt Lake City, Utah 84112.
Received July 29, 1991

Abstract: Guided ion beam mass spectrometry is used to study the reactions of ground-state Cr⁺(⁶S) with propane, butane, methylpropane, dimethylpropane, and selectively deuteriated propane and methylpropane. Thermal energy reactions of Cr⁺(⁶S) with 4-octyne are also investigated. Ground-state Cr⁺ ions undergo no bimolecular reactions at thermal energies with any of the alkanes, but do react at elevated kinetic energies. The only products formed at thermal energy in the alkane systems are the collisionally stabilized adduct complexes. Approximate lifetimes for these adducts are determined. Analyses of the endothermic processes in the alkane systems yield 298 K bond energies for several chromium–ligand species. These include the neutral and ionic chromium methyl species [$D^{\circ}(\text{Cr}-\text{CH}_3) = 37.9 \pm 2.0$ kcal/mol and $D^{\circ}(\text{Cr}^+-\text{CH}_3) = 30.3 \pm 1.7$ kcal/mol], several other chromium ion–alkyl species [$D^{\circ}(\text{Cr}^+-\text{C}_2\text{H}_5) = 35.0 \pm 2.1$ kcal/mol, $D^{\circ}(\text{Cr}^+-1-\text{C}_3\text{H}_7) = 32.1 \pm 1.4$ kcal/mol, $D^{\circ}(\text{Cr}^+-2-\text{C}_3\text{H}_7) = 28.5 \pm 1.3$ kcal/mol], and chromium ion–vinyl and –various alkylidenes [$D^{\circ}(\text{Cr}^+-\text{C}_2\text{H}_3) = 59.0 \pm 2.3$ kcal/mol, $D^{\circ}[\text{Cr}^+=\text{CHCH}_3] = 52 \pm 3$ kcal/mol, $D^{\circ}[\text{Cr}^+=\text{CHCH}_2\text{CH}_3] = 36 \pm 3$ kcal/mol, $D^{\circ}[\text{Cr}^+=\text{C}(\text{CH}_3)_2] = 39 \pm 3$ kcal/mol]. The observed reactivity requires unusual reaction mechanisms that are discussed in detail.

Introduction

Over the past decade, there has been extensive interest in examining the reactions of atomic transition-metal ions with small alkanes in order to provide insight into the means by which C–H and C–C bond activation processes might occur.^{1–6} These studies show that of the first-row transition-metal ions, Sc⁺, Ti⁺, V⁺, Fe⁺, Co⁺, and Ni⁺ undergo exothermic reactions with alkanes larger than ethane, while Cr⁺, Mn⁺, Cu⁺, and Zn⁺ do not. Often, these differences in reactivity have been attributed to thermodynamic constraints.^{3,7} This hypothesis has been tested explicitly by studies at elevated kinetic energies for Mn⁺,⁸ Cu⁺,⁹ and Zn⁺.¹⁰

For the case of Cr⁺, early studies of its reactions with butanes showed reactivity at thermal energies.¹¹ Detailed studies of the reaction of Cr⁺ with methane suggest that such thermal reactivity is due to electronically excited states of the metal ion,^{12–14} as confirmed by later studies of ground-state Cr⁺(⁶S) that found no exothermic reactions with larger alkanes, alkenes, and cycloalkanes.⁷ Schilling and Beauchamp⁷ attribute this lack of reactivity to the very weak σ bonds formed by Cr⁺, causing the insertion of Cr⁺ into C–C and C–H bonds to be endothermic. Our studies on the reactions of ground-state Cr⁺ with CH₄¹⁴ and C₂H₆¹⁵ confirmed this hypothesis and showed that the reactivity of Cr⁺(⁶S) is similar to that for the other early first-row transition-metal ions once sufficient energy is supplied to overcome the reaction endothermicities. Cr⁺ has been observed to react exothermically with 4-octyne,¹⁶ although it has not been unequivocally demonstrated that this thermal reactivity is due to the ground state. Under multicollision conditions, Cr⁺ is also seen to form colli-

sionally stabilized adduct complexes at thermal energies with CH₄, C₂H₆, and C₃H₈.¹⁷

- (1) Allison, J.; Freas, R. B.; Ridge, D. P. *J. Am. Chem. Soc.* **1979**, *101*, 1332–1333.
- (2) Allison, J. *Prog. Inorg. Chem.* **1986**, *34*, 627–677.
- (3) Armentrout, P. B.; Beauchamp, J. L. *Acc. Chem. Res.* **1989**, *22*, 315–321.
- (4) Armentrout, P. B. In *Gas Phase Inorganic Chemistry*; Russell, D. H., Ed.; Plenum: New York, 1989, pp 1–42. Armentrout, P. B. In *Selective Hydrocarbon Activation: Principles and Progress*; Davies, J. A., Watson, P. L., Liebman, J. F., Greenberg, A., Eds.; VCH: New York, 1990; pp 467–533.
- (5) Jacobson, D. B.; Freiser, B. S. *J. Am. Chem. Soc.* **1983**, *105*, 5197–5206. Buckner, S. W.; Freiser, B. S. *J. Am. Chem. Soc.* **1987**, *109*, 1247–1248. Huang, Y.; Freiser, B. S. *J. Am. Chem. Soc.* **1988**, *110*, 4434–4435.
- (6) Lebrilla, C. B.; Schulze, C.; Schwarz, H. *J. Am. Chem. Soc.* **1987**, *109*, 98–105. Schulze, C.; Schwarz, H.; Peake, D. A.; Gross, M. L. *J. Am. Chem. Soc.* **1987**, *109*, 2368–2374 and references therein.
- (7) Schilling, J. B.; Beauchamp, J. L. *Organometallics* **1988**, *7*, 194–199.
- (8) (a) Georgiadis, R.; Armentrout, P. B. *Int. J. Mass Spectrom. Ion Proc.* **1989**, *91*, 123–133. (b) Sunderlin, L. S.; Armentrout, P. B. *J. Phys. Chem.* **1990**, *94*, 3589–3597.
- (9) Georgiadis, R.; Fisher, E. R.; Armentrout, P. B. *J. Am. Chem. Soc.* **1989**, *111*, 4251–4262.
- (10) Georgiadis, R.; Armentrout, P. B. *J. Am. Chem. Soc.* **1986**, *108*, 2119–2126.
- (11) Freas, R. B.; Ridge, D. P. *J. Am. Chem. Soc.* **1980**, *102*, 7129–7131.
- (12) Halle, L. F.; Armentrout, P. B.; Beauchamp, J. L. *J. Am. Chem. Soc.* **1981**, *103*, 962–963.
- (13) Reents, W. D.; Strobel, F.; Freas, R. B.; Wronka, J.; Ridge, D. P. *J. Phys. Chem.* **1985**, *89*, 5666–5670.
- (14) Georgiadis, R.; Armentrout, P. B. *J. Phys. Chem.* **1988**, *92*, 7067–7074.
- (15) Georgiadis, R.; Armentrout, P. B. *Int. J. Mass Spectrom. Ion Proc.* **1989**, *89*, 227–247.
- (16) Schulze, C.; Weiske, T.; Schwarz, H. *Organometallics* **1988**, *7*, 898–902.

[†]Present address: Sandia National Laboratories, Division 1812, Albuquerque, NM 87185.

[‡]Camille and Henry Dreyfus Teacher-Scholar, 1987–1992.